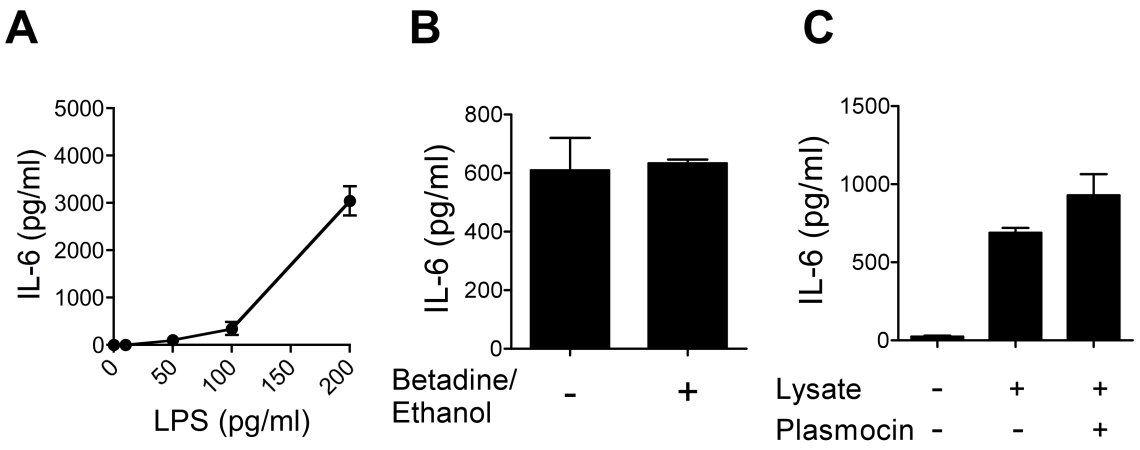

Supplemental Figure 1 Levels of LPS found within skin lysates do not activate DCs to produce IL-6.

A: IL-6 response of DCs in the presence of LPS. Concentration of LPS of <50pg/ml did not elicit an IL-6 response by DCs.

B: Treating skin with betadine/ethanol prior to skin necrosis does not diminish the IL-6 response of DCs. IL-6 concentrations were determined in cultures with DCs and skin lysates after skin was treated with betadine/ethanol.

C: IL-6 response of DCs after culture with necrotic skin lysates in the presence of plasmocin. Lysates were treated with plasmocin and then cultured with DCs. IL-6 concentrations were determined using ELISA. Experiments in A-C represent one experiment repeated independently three times with consistent results. Error bars = SEM. Assays run in triplicate in each experiment.

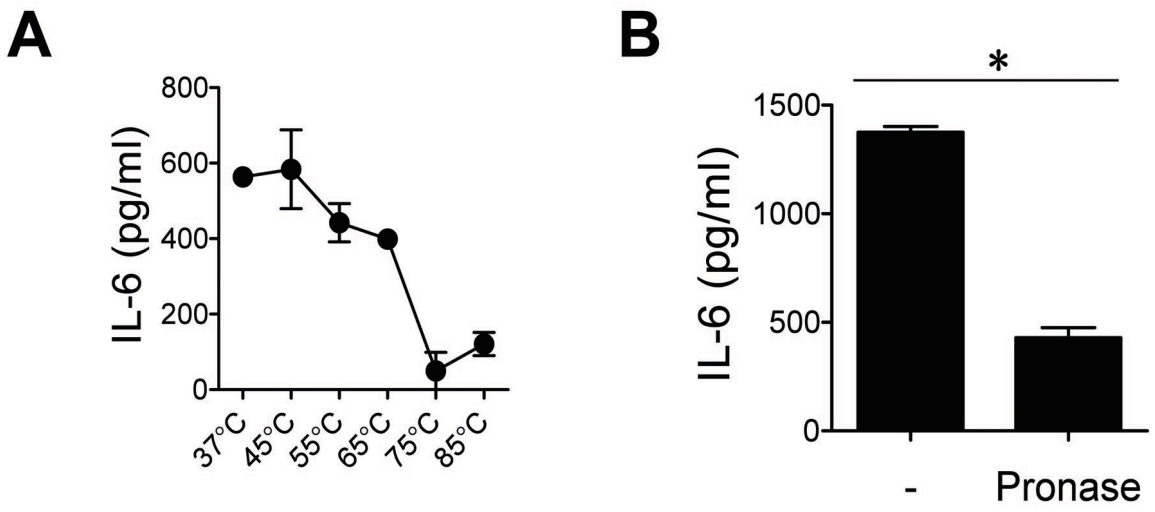

Supplemental Figure 2 Production of IL-6 in necrotic skin lysates is temperature- and protein-dependent.

A: To determine if production of IL-6 by DCs was temperature sensitive, necrotic skin lysates from non-transplanted skin were heated to the indicated temperatures and then cultured with DCs. IL-6 concentration was measured using ELISA.

B: Lysates were treated with pronase to degrade proteins, and then cultured with DCs. IL-6 was measured using ELISA.

Data in A-B are representative of one experiment repeated independently three times with consistent results. All assays run in triplicate. Error bars represent SEM.

A

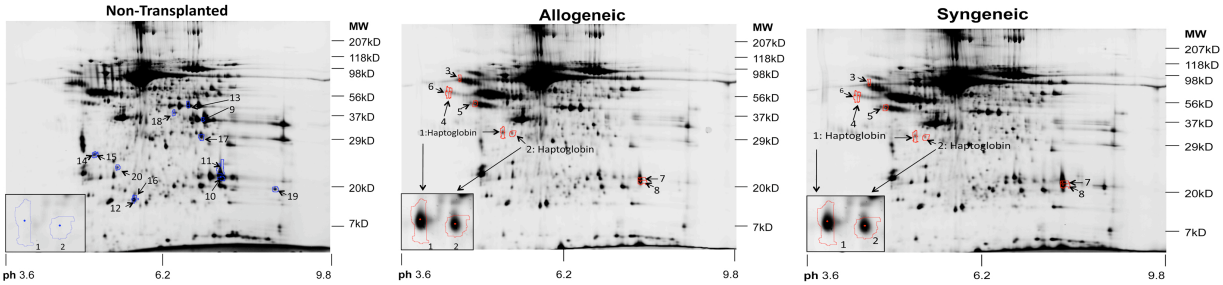

B

Matched peptides for **haptoglobin** shown in **Bold Red**

Haptoglobin Spot 1

1 MRALGAVVTL LLWGQLFAVE LGNDAMDFED DSCPKPPEIA NGYVEHLVRY
51 RCRQFYRLRA EGDGVYTLND EKQWVNTVAG EKLPECEAVC GKPKHPVDQV
101 QRIIGGSMDA KGSFPWQAKM ISRHGLTTGA TLISDQWLLT TAKNLFLNHS
151 ETASAKDITP TLTLYVGKNQ LVEIEKVVLH PNHSVVDIGL IKLKQRVLVT
201 ERVMPICLPS KDYIAPGRVG YVSGWGRNAN FRFTDRLKYV MLPVADQDKC
251 VVHYENSTVP EKKNLTSPVG VQPILNEHTF CAGLTKYQED TCYGDAGSAF
301 AIHDMEEDTW YAAGILSFDK SCAVAEYGVY VRATDLKDWV QETMAKN

Haptoglobin Spot 2

1 MRALGAVVTL LLWGQLFAVE LGNDAMDFED DSCPKPPEIA NGYVEHLVRY
51 RCRQFYRLRA EGDGVYTLND EKQWVNTVAG EKLPECEAVC GKPKHPVDQV
101 QRIIGGSMDA KGSFPWQAKM ISRHGLTTGA TLISDQWLLT TAKNLFLNHS
151 ETASAKDITP TLTLYVGKNQ LVEIEKVVLH PNHSVVDIGL IKLKQRVLVT
201 ERVMPICLPS KDYIAPGRVG YVSGWGRNAN FRFTDRLKYV MLPVADQDKC
251 VVHYENSTVP EKKNLTSPVG VQPILNEHTF CAGLTKYQED TCYGDAGSAF
301 AIHDMEEDTW YAAGILSFDK SCAVAEYGVY VRATDLKDWV QETMAKN

Supplemental Figure 3 Identification of haptoglobin in lysates by 2D-DIGE and MALDI-TOF/TOF

A: 2D-DIGE of lysates obtained from non-transplanted, syngeneic and allogeneic skin transplants (day 7 post transplantation), and labeled with cy2, cy3 and cy5 N-Hydroxysuccinimide ester dyes, respectively. MALDI-TOF/TOF identified spots 1 + 2 as haptoglobin, (inset zoom of spots shown in each gel). Spots outlined in blue (downregulated, transplanted vs. non-transplanted) / red (upregulated transplanted vs. non-transplanted) were defined by Decyder software. Identified proteins that exhibited at least a 2.5-fold change are numbered and listed in Supplemental Table 1.

B: Search results from the identification of haptoglobin protein spots 1 and 2 by MALDI-TOF/TOF and protein database searches. Sequence information was obtained from MALDI-TOF/TOF analysis of a robotically excised protein gel spot. The spots were digested using trypsin prior to analysis on an Applied Biosystems 4800 MALDI-TOF/TOF tandem mass spectometry. The data were analyzed using Applied Biosystems GPS Explorer software with the MASCOT (Matrix Science Ltd.) search engine for protein identification against the Swiss-Prot database for mouse (www.uniprot.org). In addition, a combined peptide mass fingerprint and MS/MS search was performed**.** Protein scores were 302 and 318 for spots 1 and 2, respectively (specific information regarding scores may be found at: http//www.matrixscience.com/help/interpretation_help.html).

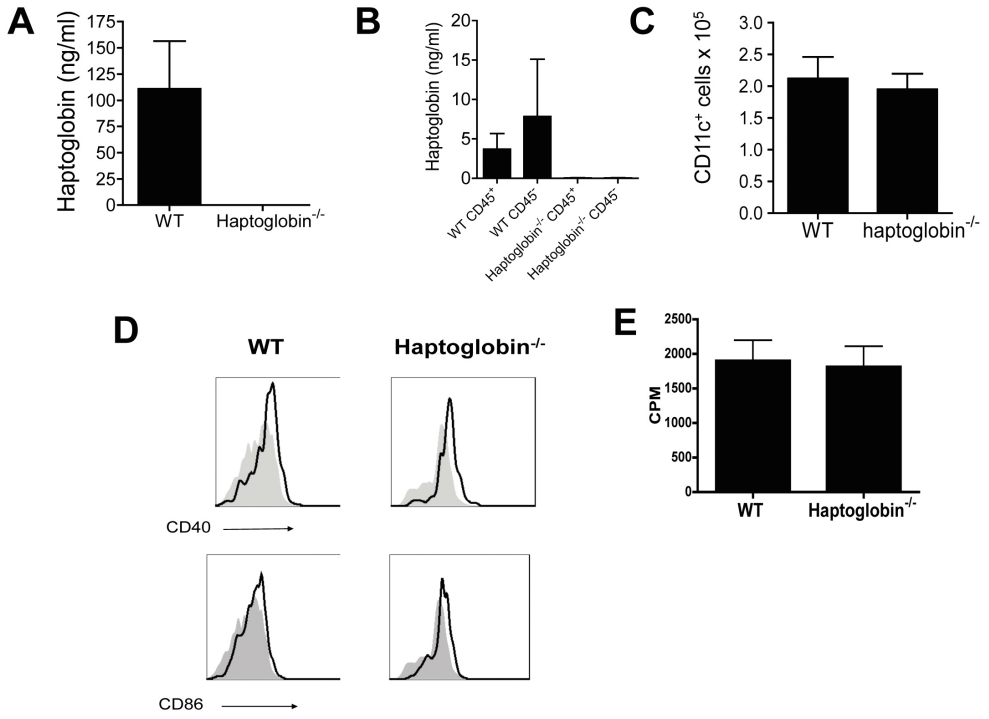

Supplemental Figure 4 Haptoglobin is present within skin. Haptoglobin deficient skin has similar numbers of CD11c$^+$ cells with similar activation status vs. CD11c$^+$ cells from WT skin.

A: Haptoglobin measured by ELISA in lysates from non-transplanted WT and haptoglobin$^{-/-}$ skin. Haptoglobin was not detected in the lysates of haptglobin$^{-/-}$skin.

B: Cells from the skin of WT and haptoglobin$^{-/-}$ non-transplanted skin were separated into lymphoid (i.e., CD45$^+$) and non-lymphoid (i.e., CD45$^-$) populations by magnetic separation, rendered necrotic and haptoglobin levels measured within each population via ELISA.

C-D: CD11c$^+$ cells were harvested from non-transplanted WT and haptoglobin$^{-/-}$ skin and enumerated via flow cytometry. **C:** Absolute numbers of CD11c$^+$ cells are shown. There were no significant differences between groups. **D**: Assessment of CD40 and CD86 expression on CD11c$^+$ cells harvested from WT and haptoglobin$^{-/-}$ non-transplanted skin by flow cytometry. Shaded histogram represents isotype control. Flow cytometric plots are gated on CD11c$^+$ cells.

E: Lymphocytes were isolated from C57BL/6 WT and haptoglobin$^{-/-}$ skin and then cultured with BALB/c T cells. Proliferation was measured after 72h culture by thymidine incorporation. T cells that were not stimulated with lymphocytes did not proliferate (not shown).

Experiments in A-E are representative of one experiment repeated independently three times with consistent results. N = 3 mice / group / experiment as a source of cells. Assays run in triplicate in each experiment, error bars = SEM

Spot#	SwissProt entry name	Mascot Score*	Protein name	Fold change vs. syngeneic	Fold change vs. allogeneic	GO Biological processes (www.geneontology.org)
1	HPT_MOUSE	302	Haptoglobin	6.53	9.97	liver development, negative regulation of hydrogen peroxide catabolic process, negative regulation of oxidoreductase activity, positive regulation of cell death, proteolysis, response to hydrogen peroxide
2	HPT_MOUSE	318	Haptoglobin	4.26	5.78	liver development, negative regulation of hydrogen peroxide catabolic process, negative regulation of oxidoreductase activity, positive regulation of cell death, proteolysis, response to hydrogen peroxide
3	SPA3K_MOUSE	397	Serine protease inhibitor A3K	3.57	5.39	negative regulation of endopeptidase activity, negative regulation of peptidase activity, regulation of proteolysis, response to cytokine stimulus, response to peptide hormone stimulus
4	SPA3M_MOUSE	543	Serine protease inhibitor A3M	3.9	3.99	negative regulation of endopeptidase activity, negative regulation of peptidase activity, regulation of proteolysis, response to cytokine stimulus, response to peptide hormone stimulus
4	SPA3K_MOUSE	332	Serine protease inhibitor A3K	3.9	3.99	negative regulation of endopeptidase activity, negative regulation of peptidase activity, regulation of proteolysis, response to cytokine stimulus, response to peptide hormone stimulus
5	A1AT1_MOUSE	152	Alpha-1-antitrypsin 1-1	4.13	4.08	acute-phase response, negative regulation of endopeptidase activity, negative regulation of peptidase activity, protein N-linked glycosylation, regulation of proteolysis, response to chromate, response to cytokine stimulus, response to lead ion, response to methanol, response to peptide hormone stimulus
6	SPA3K_MOUSE	530	Serine protease inhibitor A3K	4.43	5.54	negative regulation of endopeptidase activity, negative regulation of peptidase activity, regulation of proteolysis, response to cytokine stimulus, response to peptide hormone stimulus
7	HBA_MOUSE	322	Hemoglobin subunit alpha	6.71	3.0	erythrocyte development, in utero embryonic development, response to stilbenoid
7	HBB1_MOUSE	267	Hemoglobin subunit beta-1	6.7	3.0	erythrocyte development, hemopoiesis, oxygen transport, regulation of eIF2 alpha phosphorylation by heme
8	HBB1_MOUSE	393	Hemoglobin subunit beta-1	6.54	2.54	erythrocyte development, hemopoiesis, oxygen transport, regulation of eIF2 alpha phosphorylation by heme
9	IKCRM_MOUSE	717	Creatine kinase M-type	0.01	0.01	creatine metabolic process, phosphocreatine biosynthetic process, phosphocreatine metabolic process, phosphorylation
10	CAH3_MOUSE	347	Carbonic anhydrase 3	0.02	0.01	one-carbon metabolic process, response to oxidative stress
11	HBA_MOUSE	134	Hemoglobin subunit alpha	0.03	0.02	erythrocyte development, in utero embryonic development, response to stilbenoid
12	KAD1_MOUSE	575	Adenylate kinase isoenzyme 1	0.06	0.04	ATP metabolic process; cell cycle arrest; nucleobase, nucleoside, nucleotide and nucleic acid metabolic process; nucleotide phosphorylation; phosphorylation; positive regulation of glucose transport
12	GPX3_MOUSE	246	Glutathione peroxidase 3	0.06	0.04	glutathione metabolic process, hydrogen peroxide catabolic process, oxidation-reduction process, protein homotetramerization, response to oxidative stress
13	ENOB_MOUSE	709	Beta-enolase	0.03	0.05	glycolysis
13	ENOG_MOUSE	318	Gamma-enolase	0.03	0.05	gluconeogenesis, glycolysis
13	ENOA_MOUSE	470	Alpha-enolase	0.03	0.05	cellular response to acid; glycolysis; in utero embryonic development; metabolic process; negative regulation of cell growth; negative regulation of transcription, DNA-dependent; positive regulation of binding
14	ANXA5_MOUSE	338	Annexin A5	0.07	0.06	blood coagulation, negative regulation of coagulation, positive regulation of apoptosis, protein homooligomerization, response to organic substance
15	ANXA5_MOUSE	374	Annexin A5	0.10	0.12	blood coagulation, negative regulation of coagulation, positive regulation of apoptosis, protein homooligomerization, response to organic substance
16	GPX3_MOUSE	192	Glutathione peroxidase 3	0.13	0.14	glutathione metabolic process, hydrogen peroxide catabolic process, oxidation-reduction process, protein homotetramerization, response to oxidative stress
16	KAD1_MOUSE	497	Adenylate kinase isoenzyme 1	0.13	0.14	ATP metabolic process; cell cycle arrest; nucleobase, nucleoside, nucleotide and nucleic acid metabolic process; nucleotide phosphorylation; phosphorylation; positive regulation of glucose transport
17	ANXA1_MOUSE	177	Annexin A1	0.2	0.16	alpha-beta T cell differentiation; arachidonic acid secretion, cell cycle; cell surface receptor linked signaling pathway; cellular response to hydrogen peroxide; insulin secretion; keratinocyte differentiation; negative regulation of acute inflammatory response; negative regulation of apoptosis; negative regulation of catalytic activity; negative regulation of protein secretion; peptide cross-linking; positive regulation of apoptosis; positive regulation of prostaglandin biosynthetic process; positive regulation of vesicle fusion; regulation of cell proliferation; signal transduction
17	ALDR_MOUSE	477	Aldose reductase	0.2	0.16	Neurophysiological process_GABAergic neurotransmission
18	ACOT1_MOUSE	210	Acyl-coenzyme A thioesterase 1	0.16	0.17	acyl-CoA metabolic process, lipid metabolic process, long-chain fatty acid metabolic process
19	GSTM1_MOUSE	794	Glutathione S-transferase Mu 1	0.19	0.2	glutathione metabolic process, metabolic process
20	CLIC1_MOUSE	353	Chloride intracellular channel protein 1	0.16	0.25	chloride transport, ion transmembrane transport, ion transport, regulation of ion transmembrane transport, transport

Supplemental Table 1 List of proteins that were identified by MALDI-TOF/TOF on discovery proteomic screen in necrotic lysates of either syngeneic or allogeneic skin transplants compared to necrotic lysates of non-transplanted skin. Identified proteins that exhibited a 2.5 fold change compared to non-transplanted lysates are listed. Note, proteins may show similar migratory patterns on the 2D gel and thus >1 protein can be identified / spot. *Mascot scores refers to-10*Log(P), where P is the probability that the observed match is a random event. Proteins with the same names represented by > 1 spot correspond to isoforms.

Supplementary Methods

2D DIGE analysis protocol

Samples were solubilized into a buffer containing 7M urea, 2M thiourea and 4% CHAPS detergent with the aid of sonification (Branson model 450 sonifier with a 102C tip). Before labeling, samples were first precipitated (2D Clean-Up Kit, GE Healthcare) to rid the samples of non-protein components. Samples were then resuspended in labeling buffer containing 7M urea, 2M thiourea, 4% CHAPS (w/v) and 25 mM Tris, pH 8.6 at 4^{o}C. The samples, each containing 100 ug total protein (determined by amino acid analysis) were differentially labeled in vitro with Cy2, Cy3 and Cy5 N-hydroxysuccinimidyl ester dyes using a standard protocol (1).

For the first dimension isoelectric focusing gel, the labeled samples were pooled and mixed with 400 µL rehydration buffer containing 7M urea, 2M thiourea, 4% CHAPS weight / volume 1% DTT (weight / volume), 2% (volume / volume) pharmalytes pH 3−10 and a trace amount of bromophenol blue, and loaded onto 24 cm pH 3-10 linear IPG (immobilized pH gradient) strips by re-swelling for 3 h at 20^{o}C. Isoelectric focusing was performed on an Ettan IPGphor 3 (GE Healthcare) for approximately 60 kVh at 20°C, 50uA/strip using the following voltage gradient: (i) 11 h 30 V, (ii) 1h 500V (iii) 1h 1000V, then ~8 h linear gradient to 8000V continuing until reaching 60kVh. After focusing, IPG strips were incubated, with shaking, in an equilibration buffer containing 6M urea, 10mM Tris (pH 6.8), 30% glycerol (w/v) and 1% SDS (w/v), with 2 % (weight / volume) DTT for 15 min at room temperature. This solution was replaced with equilibration buffer containing 5% (weight / volume) iodoacetamide for an additional 10 min. For the second dimension gel, IPG strips were applied to 22 × 24 cm SDS-PAGE gels (12% T, 2.6% C).

Strips were overlaid with low melting point agarose in running buffer containing trace amounts of bromophenol blue. The gel was run at 125V (constant) and 20°C in an Ettan DALT twelve electrophoresis chamber (GE Healthcare) until the dye front had passed the bottom of the gel.

For image acquisition, gels were scanned using a Typhoon 9410 Imager (GE Healthcare). Cy2 scans were performed using a 488nm laser with a 530 nm emission filter, Cy3 images were scanned using a 532 nm laser with an emission filter of 580 nm and Cy5 images were scanned using a 633 nm laser and a 670 nm band pass 30 Hz emission filter. Photomultiplier voltage was adjusted for each channel to minimize any signal saturation. All gels were scanned at 100µm resolution, and images were further processed using ImageQuant V5.0 (GE Healthcare) prior to analyses.

Gel image analysis was performed using DeCyder v6.5, (GE Healthcare) software using the DIA (Differential in-gel analysis) analysis module. Spot detection was conducted on image pairs consisting of each sample from the same gel. These two images overlay and allowed direct measurement of volume ratios of spots between samples.

MALDI-Tof/Tof Analysis of Digests

The analysis gel was fixed in 10% methanol (volume / volume) and 7.5% acetic acid (volume / volume), post stained with Deep Purple stain (GE Healthcare) and re-scanned on the 9410 Typhoon scanner using the green (532 nm) laser, at 560 (long pass filter) emission. Spots of interest were reconfirmed and a pick list was generated and imported into the Ettan Spot Picker robot system (GE Healthcare).

Spots were subjected to robotic tryptic (Promega) digestion on a GE Healthcare Ettan TA Digester. A portion of the digest (1-1000 fmols) was desalted using a C18 ZipTip. The C-18 ZipTip (P10 size that refers to manufacturer's designated size of a polyacrylamide bead with a MW exclusion limit of 10KDa) was washed with 50% acetonitrile, 0.1% TFA (trifluoroacetic acid) and then equilibrated with 0.1% TFA (3 x 20 µl). The sample was aspirated and then expelled back into the original sample well eight times and the ZipTip was then washed 5x with 20 µl 0.1% TFA. Peptides/proteins were eluted from the ZipTip with 3 µl of 60% acetonitrile, 0.1% TFA containing 3.5 mg/ml alpha-cyano-4-hydroxy cinnamic acid matrix. 0.8ul was loaded onto the MALDI target plate. Internal calibrants, 1fmol of bradykinin (protonated, monoisotopic mass = 1060.569) and 2 fmols ACTH clip 18-39 (protonated, monoisotopic mass = 2465.199) were added with the matrix. MALDI-Tof/Tof protein identification was performed on an Applied Biosystems (AB) Model 4800 MALDI-Tof-Tof mass spectrometer. Reflectron MS analysis sums 1250 laser shots to generate the peptide fingerprint map (PFM), and the spectra were internally calibrated using the bradykinin internal standard. Masses were chosen by the AB 4000 Series Explorer software (version 3.6, Applied Biosystems) for tandem mass spectrometry (MS/MS) acquisition and extraction of the monoisotopic masses. An exclude list was used to eliminate the internal standards and trypsin autolysis fragments from MS/MS acquisition. The mass range used was 920-2500 mass / charge. MS/MS was performed first on the masses with the highest intensity, ensuring that several MS/MS spectra of good quality were obtained before the MALDI spot was depleted. Up to 10 MS/MS spectra were acquired with a minimum signal to noise threshold of 30. Fragmentation of selected precursors was performed

with the collision energy set at 2kV and atmosphere as the collision gas. 10,000 laser shots were combined for each MS/MS spectra. These were used to search for protein candidates using the UniprotKB/Swiss-Prot (IPI Mouse May 2010) and NCBI-nr (http://www.ncbi.nlm.nih.gov/blast/blast_databases.shtml>) using the MASCOT search engine (http://www.matrixscience.com). Search parameters included: allowed number of missed cleavages,1; variable modifications; methionine oxidation, carbamodomethylation. Peptide tolerance was set at +/- 20 parts per million and MS/MS tolerance at +/- 0.2 Da. Matches using mass values are handled on a probabilistic basis. The total score (denoted as MASCOT score) is the absolute probability that the observed match is a random event. Scores are reported as $-10*LOG_{10}(P)$. Only proteins that were identified by MALDI Tof/Tof and were found to be 2.5 fold changed between non-transplanted and transplanted lysates are identified on the 2D DIGE gel and listed in Supplemental Table 1.

Preparation of cells from murine skin

Cells were harvested from murine skin according to prior work (2). Mice were euthanized, fur shaved and skin washed with 95% ethanol. Trunk skin (1g) was removed and placed in a petri dish containing 0.3% Typsin/GNK solution (consisting of 0.1% glucose, 0.86% NaCl, and 0.041% KCl; epidermal surface up) for 2 h at 37°C. Skin was incubated for an additional 15 min at 37°C in 0.3% trypsin/GNK solution with DNase I (50000 Dornase units / ml, MP Biomedicals). RPMI-1640 with 10% FCS was then added to the trypsin reaction and skin cells were disaggregated by filtration through nitex nylon mesh (40μm). The cells were washed twice and used for either flow

cytometric analysis or separated into $CD45^+$ or $CD45^-$ fractions by magnetic separation (Miltenyi Biotec). For haptoglobin measurement by ELISA, $CD45^+$ or $CD45^-$ cells were rendered necrotic as previously described (3) and haptoglobin measured within lysates. To assess T cell priming function of skin lymphocytes, 1 x 10^5 lymphocytes were irradiated and cultured with 1x10^5 magnetically enriched BALB/c T cells and proliferation measured via thymidine incorporation as previously described (4).

Enzymatic protein digestion of lysates

Lysates were treated with pronase (Calbiochem-Behring Corp) at 37°C for 1 h and then at 59°C for 10 min to degrade proteins.

References

1. Wu, T. 2006. Two Dimensional Difference Gel Electrophoresis. In *New and Emerging Proteomics Techniques* D. Nedelkov, Nelson, R.W.,, editor: Human Press Inc.

2. Gao, Y., Yang, W., Pan, M., Scully, E., Girardi, M., Augenlicht, L.H., Craft, J., and Yin, Z. 2003. Gamma delta T cells provide an early source of interferon gamma in tumor immunity. *J Exp Med* 198:433-442.

3. Sauter, B., Albert, M.L., Francisco, L., Larsson, M., Somersan, S., and Bhardwaj, N. 2000. Consequences of Cell Death. *J Exp Med* 191:423-434.

4. Shen, H., and Goldstein, D.R. 2009. IL-6 and TNF-{alpha} Synergistically Inhibit Allograft Acceptance. *J Am Soc Nephrol* 5:1032-1040.